

Regular article

Dimer models for ErbB-2/neu transmembrane domains from molecular dynamics simulations*

Nicolas Sajot, Norbert Garnier, Monique Genest

Centre de Biophysique Moléculaire, UPR 4301 CNRS, affiliated to the University of Orleans,
Rue Charles Sadron, F-45071 Orléans Cedex 02, France

Received: 24 April 1998 / Accepted: 17 September 1998 / Published online: 10 December 1998

Abstract. Interest in the transmembrane receptors tyrosine kinase of the erbB family is high due to the involvement of some of the members in human cancers. The original oncogenic alleles of neu discovered in rat neuroectodermal tumors lead to single Val664Glu substitution within the predicted transmembrane domain. Identical substitution at the homologous position 659 constitutively activates the oncogenic potential of the human ErbB-2 receptor by enhanced receptor dimer formation. The precise molecular details of receptor dimerization are still unknown and to acquire more knowledge of the mechanisms involved, molecular dynamics simulations are undertaken to study transmembrane dimer association. Transmembrane helices are predicted to associate in left-handed coiled-coil structures stabilized by Glu-Glu interhelix hydrogen bonds in the mutated form. The internal dynamics reveals π helix deformations which modify the helix-helix interface. Predicted models agree with those suggested from polarized IR and magic-angle spinning NMR spectroscopy.

Key words: ErbB-2/neu transmembrane domains – Molecular dynamic simulations – Helix-helix association – π helix deformations

1 Introduction

Membrane receptors are activated through ligand-induced receptor dimerization or oligomerization. For tyrosine kinase receptors of the erbB family that are anchored in the membrane with a single transmembrane

(TM) domain, dimerization appears as a general mechanism for receptor activation [1]. The increased number of normal receptors – overexpression – is often involved in various human tumor cells [2] and aberrant activation of kinase activity is directly linked to tumorigenesis. A Val-Glu mutation in the TM region of the homologous neu protein is shown to be responsible for dimerization and for constitutive kinase activation linked to the transforming potential of the activated neu protein [3]. This same mutation induced in the human ErbB-2 TM domain results in cellular transformation without ligand stimulation [4, 5].

This discovery of ligand-independent dimerization of oncogenic ErbB-2/neu has led to extensive studies to explain the role of the critical function of the specific point mutation Val659/664 which constitutively activates the intrinsic tyrosine kinase and results in cellular transformation. The TM packing region was strongly suggested to play an active role in dimerization [6]. Site-directed mutagenesis studies demonstrate that both dimerization and transformation are dependent on a domain formed by the local environment proximal to the critical Glu transforming residue [7–9]. The tripeptide structure VEG was first suggested to be sufficient for the effect of Glu664 [8]. However, movement of the VEG triplet within the TM domain leads to mutants that dimerize well but fail to transform [10, 11].

This high interreceptor contact point is shown to be necessary for dimerization but is not sufficient to explain transformation and it is supposed that other secondary interactions cooperate resulting in helix contact [10].

One approach to the rational design of TM domain recognition is the use of molecular simulation. Using the assumption of independently stable TM helices [12], one can hope to pack ErbB-2/neu TM helices to understand the mechanism of induction of dimerization by Glu mutation. This is of great interest because of the potential use of TM peptides to interfere with signaling [13].

We present the best models of ErbB-2/neu dimers in both wild and oncogenic forms obtained from molecular dynamics (MD) simulations, showing that the two hel-

* Contribution to the Proceedings of Computational Chemistry and the Living World, April 20–24, 1998, Chambéry, France

Correspondence to: M. Genest
e-mail: geneste@cns-orleans.fr,
Tel.: +33-2-38257668, Fax: +33-2-38631517

ices associate in a left-handed supercoil and that most of the interfacing residues are the conserved residues between the two sequences.

2 Computational modeling

The same computational approach as previously developed for the study of ErbB-2 TM helix dimer [14] was applied in the search for the most stable dimers of both wild and oncogenic neu TM. The 25-residue sequence of the TM domain extending from Leu651 to Ile675 for ErbB-2 and from Val656 to Ile680 for neu are used in this study. Position 9 in the peptide sequence is the position Val659/664 of the mutation site of the entire neu/ErbB-2 receptors.

The global search of low-energy configurations of interacting helices was carried out in two steps. The first step was to roughly determine the distance of approach for two parallel identical helices. This was done by rotating each helix (θ_H angle), considered as a rigid body, about its own helical axis for a complete revolution (0° , 360°) in intervals of 18° in order to examine all the helix-helix interfaces. For each of the 441 configurations generated defined by $(\theta_{H1}, \theta_{H2})$, all the non-bonded interactions were evaluated by summing the van der Waals and the electrostatic energies using the parameters of the GROMOS force field [15] and a relative dielectric constant of 1. This rapid search of all interacting faces was repeated for several distances of separation between the two helical axes ranging from 0.9 to 1.2 nm for each TM dimer type. The shorter distance D_H for which no dramatic clashes are detected overall is 1.07 nm for the ErbB-2 TM dimer and 1.11 nm for the neu TM dimer for both types of TM.

In a second step, the conformational space of two interacting TM helices placed parallel and separated by D_H was examined more closely by calculating all atomic interactions by employing the complete GROMOS force field with the same relative dielectric constant value. The total potential energy of each configuration, expressed as the sum of the potential energy of each helix and the intermolecular energy between the two helices, was energy-minimized for several hundred steepest descent steps. No constraint of distance of separation or backbone hydrogen bond (HB) was applied, allowing both helices to move freely. The low-energy configurations were then extracted from the minimized potential energy surface.

This process, repeated for both neu and ErbB-2 TM in the wild and the oncogenic forms, allowed a common low-energy configuration characterized by the presence of the mutation site at the helix-helix interface to be identified. This configuration is particularly interesting since it defines an interface very close to that suggested by Sternberg and Gullick [6] from stereochemical models in which the facing Glu side chains have been hypothesized to form interhelix HBs.

Starting from this configuration, multiple simulations were carried out using different initial random velocities in each case. The heating period was produced by successive temperature stages of 50 K applying atomic ve-

locity rescaling. Constant temperature was maintained by a heat bath [16] with a strong coupling constant up to 300 K. Weak coupling was applied for equilibration and production periods over a total duration of 840 ps. Bond lengths were not constrained (SHAKE not applied) and a time step of 0.0005 ps was used. MD simulations were carried out in vacuum employing the same force field without interaction truncations. The core of the membrane, essentially constituted of hydrocarbon chains, is a low dielectric constant medium and in vacuum simulations may provide a reasonable first approximation to helix dimerization within a bilayer as exemplified by studies on glycoporphin A [17, 18]. As in the minimization step, no restraints were applied to maintain the α -helical conformation and helix-helix separation and no assumption about helix-helix association was made. Helices were allowed to move freely for packing optimization.

The final coiled-coil structures are characterized by the crossing-angle value defined by the dihedral angle between the two helix axes. The helix axis was described by the principal long axis calculated from the atomic coordinates of each helical backbone. The definition of the crossing angle is that given by Chothia et al. [19].

The helicity of each monomer probed by the backbone HB network and HBs between the two helices is followed all along the simulations. The existence of a HB depends on the following distance and angle criteria: donor(D)-acceptor(A) less than 0.35 nm and DHA angle between 130° and 180° .

3 Preference for left-handed super coiling of ErbB-2/neu TM

Of ten structures generated, eight are characterized by a crossing-angle value ranging an average from 25° to 43° over the last 100 ps of the simulation indicating a strong preference for left-handed supercoiling. Two other structures were found in a slightly right-handed supercoil with a crossing angle of about -5° and, at this stage of the study, this result does not rule out the existence of right-handed structures or transitions toward left-handed structures on a longer time scale.

Time series of crossing angles for the four structures the wild and oncogenic ErbB-2 dimer and the wild and oncogenic neu dimers are given in Fig. 1 and illustrate how the dimer structures evolve with time. The final left-handed structure is reached along different pathways depending on the TM sequences. For ErbB-2 dimers, the left-handed structure is established during the heating period and, for the oncogenic type, the structure is maintained all along the simulation. For the wild type, the structure is stabilized after 500 ps during which the supercoil largely fluctuates showing transitions between the left sense and the right sense of the helix winding. Both wild and oncogenic dimers are stabilized in a left-handed structure with a crossing angle of 25° and 27° , respectively. These values are calculated for the average structures over the last 100 ps of the simulation.

The neu dimers behave differently than the ErbB-2 dimers. Corresponding plots show clearly that transi-

tions between right-handed and left-handed supercoils occur. In the wild case, a value of -20° is reached for short periods of time. The left-handed structure stabilizes at about 600 ps in both cases. The average structures of the wild and oncogenic dimers calculated over the last 100 ps of the simulation cross at 43° and 33° , respectively. For these two neu dimers, the crossing angle is higher than for ErbB-2, suggesting a different helix-helix packing.

4 Helicity and interhelix HBs

Time series of the backbone HB network registered for each simulation reveal that the α -canonical helix struc-

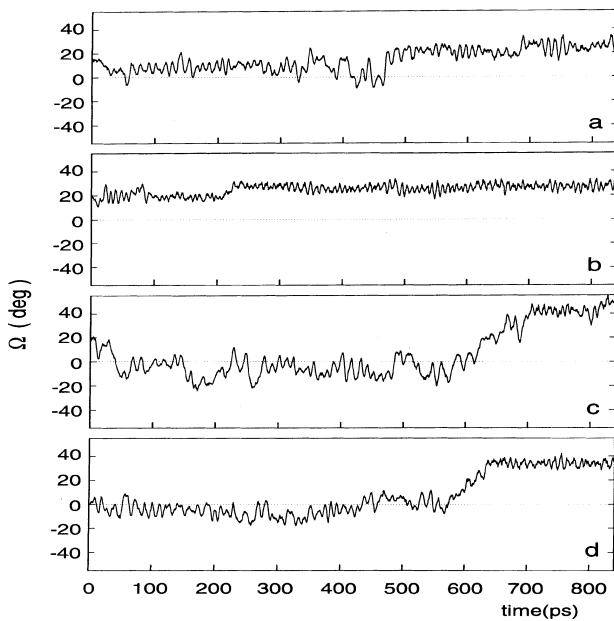


Fig. 1a-d. Time series of the crossing angle for ErbB-2 dimers, **a** wild, **b** oncogenic, and for neu dimers, **c** wild and **d** oncogenic

ture is not completely maintained. Helix deformations occur while TM helices associate and, as already described for isolated ErbB-2 TM [20, 21], correspond to conversion of α -helix portions to π -helix portions. π i , $i + 5$ HB detected in helix H1 and helix H2 for the minimized average structures of ErbB-2/neu dimers are reported in Table 1. The detailed analysis of π -HB formation indicates that the appearance of i , $i + 5$ HB followed by their propagation along the helix coincides with crossing-angle variations. Clearly, π -helix formations induce changes in the supercoils. This is particularly well evidenced for the neu dimer structures where successive π HB are detected both in H1 and H2 for the wild type or only in H2 for the oncogenic type. The mutation region is sensitive to π transitions and it is found for both cases in helix H2. The high value of the crossing angle seen for the wild type is probably due to helix deformations occurring at two distinct regions both in helix H1 and helix H2.

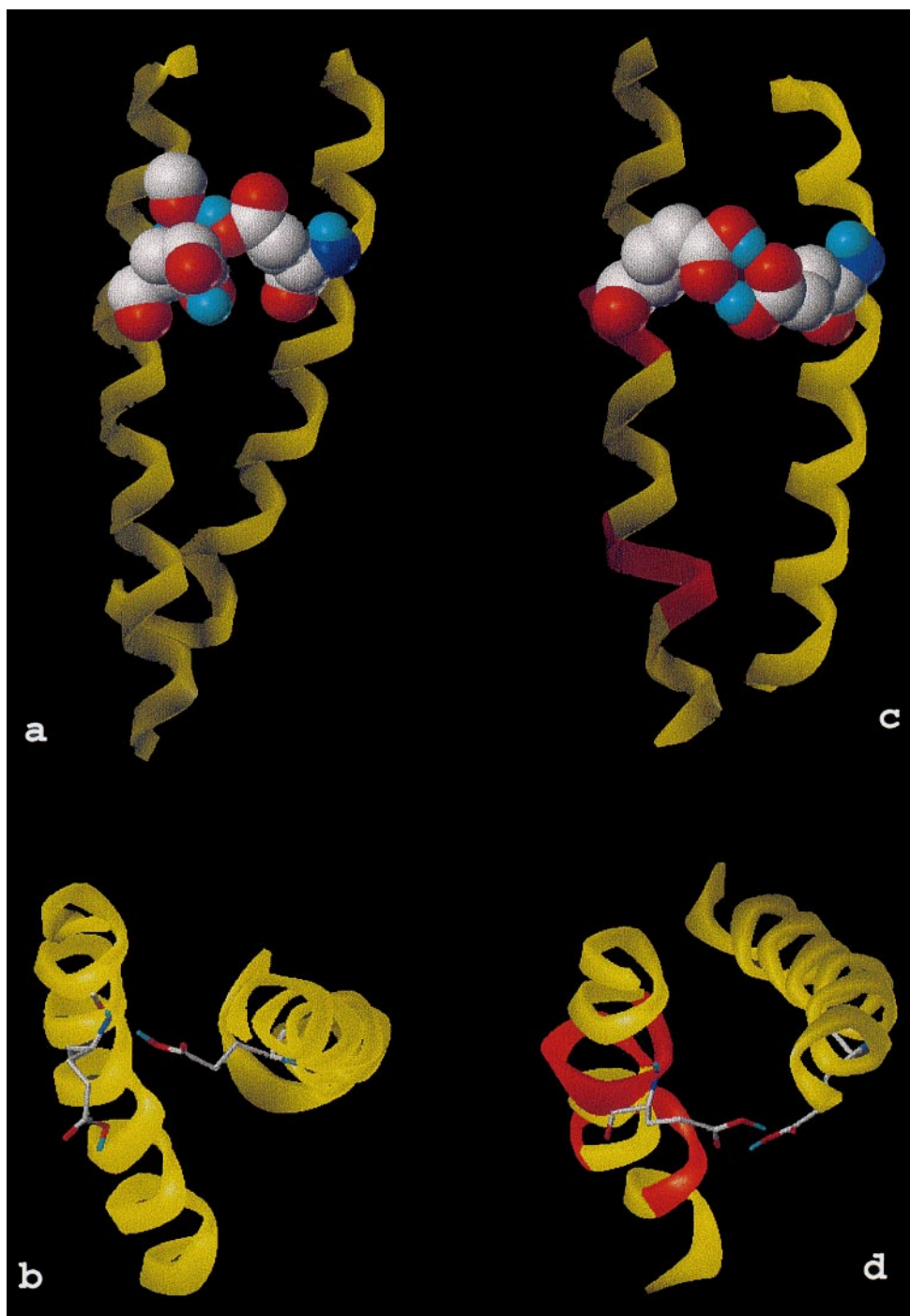
For the ErbB-2 wild type, the i , $i + 5$ HB pattern is less extended and the deformation affects only one helix. π -HB appearance immediately induces an increase in the crossing angle. The oncogenic form does not exhibit such helical deformation during the time scale examined. Undistorted α -helical structures account for a stable left-handed supercoil in that case.

Examination of HBs formed between the two helices evidences that the protonated Glu side chains are involved in helix-helix interactions. For the oncogenic neu dimer, symmetrical carboxyl Glu-Glu side chains are observed, whereas for ErbB-2, only the Glu side chain of H1 is hydrogen-bonded to the facing CO Ile4 of helix H2, still involved in the α -HB network. A view of these structures is given in Fig. 2. In addition, the hydroxyl groups of Ser and Thr residues at the N-terminus are linked to carbonyl groups of the facing residues by HB interactions. These interhelix HBs are not maintained for the entire simulation. They are established transiently and are seen for some of them at a significant residence time for the last 100 ps. Simulations continued on

Table 1. Crossing-angle values for the left-handed structures of ErbB-2/neu dimers and hydrogen bonds in the helix backbone (i , $i + 5$ π type) and between the two helices

Crossing angle	ErbB-2 dimers				neu dimers			
	wild		oncogenic		wild		oncogenic	
	H1	H2	H1	H2	H1	H2	H1	H2
	25°		27°		43°		33°	
Hydrogen bonds CO ₇ -NH _{i+5}		T2-A7 S3-V8		V20-I25	L15-V20 I16-V21	I4-V9 I5-G10 A6-V11 T7-L12 V8-L13		I4-E9 I5-G10 A6-V11 T7-L12 V8-L13
		G10-V15 I11-V16 L12-L17 L13-G18			V18-I23 V19-L24 V20-I25	V18-I23 V19-L24 V20-I25		L15-V20 I16-V21 L17-G22
Interhelix hydrogen bonds	S6O ₇ H-I4CO		E9O ₈ 2H-I5CO					E9O ₈ 1-E9O ₈ 2H E9O ₈ 2H-E9O ₈ 1 E9O ₈ 2-E9O ₈ 2H

Fig. 2. Dimer models for oncogenic ErbB-2 (**a** and **b**) and neu (**c** and **d**) transmembrane domain. The α helix is colored in *yellow* and the π -helix portions are colored in *red*. Glu side chains show two types of interactions: side chain–backbone (oncogenic ErbB-2: **a**) and side-chain–side-chain (oncogenic neu: **b**). Images **b** and **d** are rotated by 90° and show how helices are wrapped around each other with the Glu side chains at the helix-helix interface. Helix H1 is on the right, helix H2 is on the left in the four images



a longer time scale (not shown) show that hydroxyl groups fluctuate between inter- and intra-HB interactions with carbonyl groups of their own helix and with those of the facing helix, respectively. For the oncogenic ErbB-2 dimer, the dynamics of the Glu side chains brings the carboxyl extremity in a favorable position for symmetrical HBs as observed for the neu dimer.

These structures agree well with the first model suggested by Sternberg and Gullick [6] supporting the proposal of stabilizing Glu-Glu side chain interactions or Glu-carbonyl backbone HB interactions between the two TM helices. Such helix-helix association reinforced

by symmetrical Glu-Glu side chain interactions was recently suggested by polarized IR and magic-angle spinning NMR studies [22]. In addition, it is proposed that the left-handed structure allows such interactions.

Our simulations demonstrate that the transforming mutation induces highly specific interactions between helices for both ErbB-2/neu dimers. Packing of helices driven by van der Waals interactions for the wild type is strongly maintained by additional electrostatic interactions due to hydrophilic mutation. Interhelix interaction energies including van der Waals and electrostatic interactions are stronger for the oncogenic type than for

the wild type. A gain of 52 kJ/mol for the ErbB-2 dimer and 97 kJ/mol for the neu dimer evidences the stabilizing role of the transforming Glu mutation.

5 Helix-helix interface

Contacting residues are given in Table 2 and show that the two helices are in close contact for the total length. Undistorted α helices of the oncogenic ErbB-2 dimer exhibit an intimate interface by packing side chains of helix H1 into spaces between the facing side chains of helix H2. The two helices crossed at an angle of 27° is the Crick model [23] proposed to stabilize a left-handed supercoil. At the mutation site the Glu side chains are in close proximity as seen in Fig. 2. The VEG triplet is present at the interface and the two other Gly residues comprise the C-terminal interface with Val and Leu facing residues.

This regular packing of the two α helices is modified under the effect of local short π -helix appearance. In the wild ErbB-2 dimer, the π deformation detected in H2 in its second moiety rotates the interfacing residues of one position by about 100° around the helix axis. The same residues of H1 -Val16, Val20, Ile23- have their side chains sandwiched by the Leu17-Val16, Val20-Val19, and Leu24-Ile23 pairs, respectively. The two following Gly residues are rotated off the interface and are replaced by the larger side chains of Val and Ile residues allowing a more compact interface. The regular side-chain packing which consists of one side chain of one helix between two other side chains of the other helix is observed in this structure. For the neu dimers, the much more deformed helices result in a slightly different side chain assembly. π stretches do not cover the same short sequences in the wild and oncogenic dimer and a different helix-helix interface is formed. For the wild dimer which has two much more twisted helices the Gly10 residue is not at the interface.

Although these four structures do not converge to a unique helix-helix packing, it is of interest to analyze the contacting side chains. These define six anchoring points

at the interface (Table 2). Slight distortions at the N-terminus of the helices modulate the interhelix interactions at this level, but for each of the structures Thr2 of helix H1 stands at the helix-helix interface and participates in dimer stabilization by HB interactions between its hydroxyl group and carbonyl groups of the first residues of helix H2.

The first anchoring point reported in Table 2 includes the small Ser6/Ala6 side chain facing two Ile residues. Then at the mutation site, the Val/Glu9 side chain fills the space between the facing Val8 and Val9/Glu9. A Leu rich contact constitutes the fourth anchoring point, and this position corresponds to conserved Leu residues of ErbB-2/neu TM sequences. The following anchoring point is more diversified, but the same position Val/Ile16 is observed at the interface. At the C-terminal of the supercoil the interface shows a Val rich contact followed by a Leu/Ile rich point which are the conserved residues between both the neu and ErbB-2 TM sequences.

6 Conclusion

The propensity for ErbB-2/neu TM dimers to form left-handed helical supercoils emerges from our simulations. Our results show that the VEG triplet constitutes a strong nucleation point for dimerization where the side chain of the mutation site is intimately packed between that of its cognate and the proximal Val residue. Most of the conserved residues between the neu and ErbB-2 TM are present at the helix-helix interface.

The non-canonical α helices predicted from our simulations do not allow to draw clear rules for helix assembly. However, our result supports the fact that hydrophobic interactions contribute to stability, and the hydrophilic Glu interactions introduce specificity. Our predicted models for ErbB-2/neu TM helix-helix association are in a complete accord with the model suggested from experimental data [22]. The left-handed supercoil is consistent with statistical analysis showing that it is the prevalent structure in which TM helices

Table 2. Helix-helix interface for the ErbB-2/neu transmembrane dimer models

ErbB-2 wild	I5		V9	L12		L17	V19		L24		
	S6	I5	V9	V8	L13	L12	V16	V16	V20	I23	I23
ErbB-2 oncogenic		I4	G10			I11	L17		V19	L24	
	I5	I5	E9	E9	L12	L12	V16	V16	V19	V19	I23
neu wild	S6	I4	G10	V8	L13	I11	L17	V15	V20	G18	L24
		I5	V8	V9	L12	L13	L15		V20	L24	
neu oncogenic	A6	I4	V9	V8	L13		I16	L15	V19	V19	I23
		I5		E9		L13	L13	I16		V20	I23
neu oncogenic	A6	I4	E9	V8	L13	L12	L17	I16	V20	V19	L24
	T7		G10		F14			L15	V21		G22

achieve efficient packing [24, 25]. Our modeling approach provides a valuable starting point for understanding dimerization mediated by the TM domains of ErbB receptors.

References

1. Heldin CH (1995) *Cell* 80:213–223
2. Hynes NE, Stern DF (1994) *Biochim Biophys Acta* 1198:165–184
3. Bargmann CI, Hung MC, Weinberg RA (1986) *Cell* 45:649–657
4. Masuko T, Sugahara K, Kozono M, Otsuki S, Akiyama T, Yamamoto T, Toyoshima K, Hashimoto Y (1989) *Jpn J Cancer Res* 80:10–14
5. Segatto O, King CR, Pierce JH, Di Fiore PP, Aaronson SA (1988) *Mol Cell Biol* 8:5570–5574
6. Sternberg MJ, Gullick WJ (1989) *Nature* 339:587
7. Bargmann CI, Weinberg RA (1988) *EMBO J* 7:2043–2052
8. Cao H, Bangalore L, Bormann BJ, Stern DF (1992) *EMBO J* 11:923–932
9. Sternberg MJ, Gullick WJ (1990) *Protein Eng* 3:245–248
10. Burke CL, Lemmon MA, Coren BA, Engelman DM, Stern DF (1997) *Oncogene* 14:687–696
11. Chen LI, Webster MK, Meyer AN, Donoghue DJ (1997) *J Cell Biol* 137:619–631
12. Popot JL, Engelman DM (1990) *Biochemistry* 29:4031–4037
13. Lofts FJ, Hurst HC, Sternberg MJ, Gullick WJ (1993) *Oncogene* 8:2813–2820
14. Garnier N, Genest D, Duneau JP, Genest M (1997) *Biopolymers* 42:157–168
15. van Gunsteren WF (1987) GROMOS, Groningen Molecular Simulation System. BIOMOS Biomolecular Software, Groningen, Germany
16. Berendsen HJC, Postma JPM, van Gunsteren WF, Dinola A, Haak JR (1984) *J Chem Phys* 81:3684–3690
17. Treutlein HR, Lemmon MA, Engelmann DM, Brünger AT (1992) *Biochemistry* 31:12726–12733
18. Lemmon MA, Treutlein HR, Adams P, Brünger AT, Engelman DM (1994) *Nat Struct Biol* 1:157–163
19. Chothia C, Levitt M, Richardson D (1981) *J Mol Biol* 145:215–250
20. Duneau JP, Genest D, Genest M (1996) *J Biomol Struct Dyn* 13:753–769
21. Duneau JP, Garnier N, Genest M (1997) *J Biomol Struct Dyn* 15:555–572
22. Smith SO, Smith CS, Bormann BJ (1996) *Nat Struct Biol* 3:252–258
23. Crick FHC (1953) *Acta Crystallogr* 6:689–697
24. Bowie JU (1997) *Nat Struct Biol* 4:915–917
25. Bowie JU (1997) *J Mol Biol* 272:780–789